

Enhancing the safety of ovarian cortex autotransplantation: cancer cells are purged completely from human ovarian tissue fragments by pharmacological inhibition of YAP/TAZ oncoproteins

Callista L. Mulder^{1,2}, Lotte L. Eijkenboom¹,
Catharina C.M. Beerendonk¹, Didi D.M. Braat¹, and Ronald Peek^{1,*}

¹Radboud University Medical Center, Department of Obstetrics and Gynecology, PO Box 9101, 6500 HB, Nijmegen, The Netherlands

²Current address: Amsterdam UMC, University of Amsterdam, Center for Reproductive Medicine, Amsterdam Reproduction and Development Research Institute, Reproductive Biology Laboratory, Meibergdreef 9, 1105 AZ Amsterdam, The Netherlands.

*Correspondence address. Radboud University Medical Center, Department of Obstetrics and Gynecology, Nijmegen, The Netherlands.
E-mail: Ronald.Peek@Radboudumc.nl.

Submitted on August 9, 2018; resubmitted on October 22, 2018; accepted on December 4, 2018

STUDY QUESTION: Is it possible to eliminate metastasized cancer cells from ovarian cortex fragments prior to autotransplantation without compromising the ovarian tissue or follicles?

SUMMARY ANSWER: Ex vivo pharmacological inhibition of YAP/TAZ by Verteporfin enabled us to efficiently eradicate experimentally induced small tumours, derived from leukaemia and rhabdomyosarcoma, from human ovarian tissue fragments.

WHAT IS KNOWN ALREADY: Autotransplantation of ovarian tissue fragments that contain metastasized tumour cells may reintroduce the malignancy to the recipient. In order to enhance safety for the patient there is a strong need for protocols that effectively purges the ovarian tissue from malignant cells ex vivo prior to transplantation, without compromising ovarian tissue integrity.

STUDY DESIGN, SIZE, DURATION: Tumour foci were experimentally induced in human ovarian cortex tissue fragments derived from at least three patients by micro-injection of cancer cell lines. Next, the tissue fragments were cultured to allow formation of metastasis-like structures followed by a 24 h ex vivo treatment with the YAP/TAZ inhibitor Verteporfin to eradicate the cancer cells. A control treatment was included in all experiments. The purged ovarian cortex fragments were cultured for an additional 6 days to allow any possibly surviving cancer cells to establish new metastatic foci.

PARTICIPANTS/MATERIALS, SETTING, METHODS: Human ovarian tissue was obtained after female-to-male sex reassignment surgery. Human rhabdomyosarcoma, leukaemia, breast cancer and Ewing's sarcoma cell lines were utilized for the induction of tumour foci. Tumour specific (immuno)histochemistry and RT-PCR were used for the detection of residual cancer cells after ex vivo treatment. Ovarian tissue and follicle integrity after exposure to Verteporfin was evaluated by histology, a follicular viability assay and a glucose uptake assay.

MAIN RESULTS AND THE ROLE OF CHANCE: Metastasized rhabdomyosarcoma and leukaemia cells could be effectively purged from ovarian cortex tissue by a 24 h ex vivo treatment with Verteporfin, while breast cancer and Ewing's sarcoma did not respond to this treatment. Ovarian tissue integrity was not affected by purging, as no statistically significant difference ($P > 0.05$) was observed in the percentage of morphologically normal follicles, percentage of follicles with apoptotic cells, follicular viability or glucose uptake between the control treated ovarian cortex and Verteporfin treated ovarian cortex.

LIMITATIONS, REASONS FOR CAUTION: Our tumour model is based on growth of human cancer cell lines. It is unclear whether these cells reflect the behaviour of malignant cells that have metastasized to the ovary during natural disease progression. Furthermore, the functionality of the ovarian tissue after ex vivo treatment requires further investigation *in vivo*.

WIDER IMPLICATIONS OF THE FINDINGS: The results indicate that ex-vivo tumour cell purging of human ovarian cortex fragments intended for fertility preservation purposes is feasible by short-term pharmacological treatment. Effective purging of the ovarian cortex tissue enhances safety of ovarian cortex autotransplantation for the patient. This increases the likelihood that this form of fertility restoration may become an option for patients with malignancies for which ovarian cortex transplantation is currently considered unsafe.

STUDY FUNDING/COMPETING INTEREST(S): Unconditional funding was received from Merck B.V. The Netherlands (Number 2016-FERT-1) and the foundation 'Radboud Oncologie Fonds' (Number KUN 00007682). The authors have no conflicts of interest.

TRIAL REGISTRATION NUMBER: NA.

Key words: oncofertility / safety / ovarian cortex / Verteporfin / YAP/TAZ / purging

Introduction

When young girls and women of reproductive age are diagnosed with cancer, they not only face burdensome cancer therapy, but also the threat of future subfertility due to gonadotoxicity of the majority of anti-cancer regimens (Wallace *et al.*, 2005; Levine, 2012; Donnez and Dolmans, 2017). For prepubertal girls and women that require immediate cancer treatment cryopreservation of ovarian cortex is the sole option to secure their fertility (Dolmans, 2018). Once the patient is cured and wishes to conceive, she can opt for autotransplantation of the cryopreserved ovarian tissue (OCT). The tissue is thawed and preferably transplanted to the remaining ovary, where small immature follicles resume follicular development, allowing the patient to conceive naturally or with the aid of IVF. In 2004, the first children were born after transplantation of (cryopreserved) ovarian tissue (Donnez *et al.*, 2004; Meirow *et al.*, 2005; Silber *et al.*, 2005) and since then 130 live births have been reported from autotransplantation of ovarian cortex tissue worldwide (Donnez and Dolmans, 2017).

Even though OCT has proven its effectiveness in restoring fertility in female cancer survivors (Jensen *et al.*, 2017; Dolmans, 2018; Schuring *et al.*, 2018; von Wolff *et al.*, 2018), the potential contamination of the ovarian tissue with malignant cells remains a major concern. Ovarian tissue is ideally obtained prior to the administration of radio- or chemotherapy and may therefore contain metastasized cancer cells. Moreover, ovarian tissue from chronic myeloid leukaemia (CML) and acute lymphoblastic leukaemia (ALL) patients was capable of inducing tumours upon xenotransplantation to immunodeficient mice (Dolmans *et al.*, 2010).

Ideally, the ovarian tissue to be transplanted should be screened for the presence of tumour cells. This screening may be performed by immunohistological analysis (Azem *et al.*, 2010) either in combination with tumour-specific polymerase chain reaction (PCR) examination of the tissue (Rosendahl *et al.*, 2010) or xenotransplantation and next generation sequencing (Shapira *et al.*, 2018). However, these approaches not do confirm the absence of malignant cells in the tissue that is actually transplanted, since the analysed fragment is no longer available for transplantation purposes. Alarmingly, cortex tissue fragments from the same ovary of a cancer patient may give different results when analysed by a tumour-specific RT-PCR (Rosendahl *et al.*, 2010), indicating that analysis of only a small part of the cortex

fragments may yield results that are not representative for the remaining tissue fragments.

Several alternative approaches to prevent cancer reintroduction by autotransplantation of ovarian cortex tissue are currently under investigation, including maturation of primordial follicles *in vitro* (McLaughlin *et al.*, 2018) or incorporating isolated follicles in an artificial ovary (Chiti *et al.*, 2018). However, these options are currently not yet available for clinical use. Another alternative strategy is eradication of malignant cells from the isolated ovarian cortex tissue fragments prior to autotransplantation (Schroder *et al.*, 2004). Tumour cell purging by ex vivo treatment of human grafts before transplantation has been performed in other procedures such as hematopoietic stem cells transplantation in breast cancer patients (Leone *et al.*, 2006), patients with neuroblastoma (Kreissman *et al.*, 2013), or patients with multiple myeloma (Bartee *et al.*, 2012). These approaches have been shown to result in a statistically significant lower chance of relapse after transplantation (Yahng *et al.*, 2014). Since the ovarian tissue needs to remain intact, the use of cell sorting is not an option for purging of ovarian cortex tissue. We therefore applied pharmacologic ex vivo purging of the ovarian cortex tissue.

The ideal ex vivo purging protocol would involve pharmacologic eradication of cancer cells derived from various malignancies. The inhibitory molecules should be small enough to allow for efficient penetration into the cortex tissue in the absence of perfusion. To safeguard the condition of the ovarian cortex tissue, it is crucial that the purging procedure does not impair follicular function or damage the ovarian stromal cells. A plausible target for the ex vivo treatment of cortex tissue is the Hippo pathway (also known as the Salvador-Warts-Hippo Pathway). This kinase cascade has been shown to be deregulated in a wide variety of human malignancies (Harvey *et al.*, 2013) and has been suggested to play only a minor role in normal physiological adult tissue homeostasis (Wang *et al.*, 2017). The cascade leads to the inactivating phosphorylation of the central mediators in this pathway, Yes-associated protein (YAP) and transcriptional co-activator with PDZ-binding motif (TAZ). YAP and TAZ oncproteins have been shown to play a pivotal role in tumorigenesis, and confer malignancy and drug resistance to a variety of tumours including breast cancer (Bartucci *et al.*, 2015), (rhabdomyo)sarcoma (Slemmons *et al.*, 2015; Fullenkamp *et al.*, 2016), leukaemia (Li *et al.*, 2016) and Ewing sarcoma (Ahmed *et al.*, 2015).

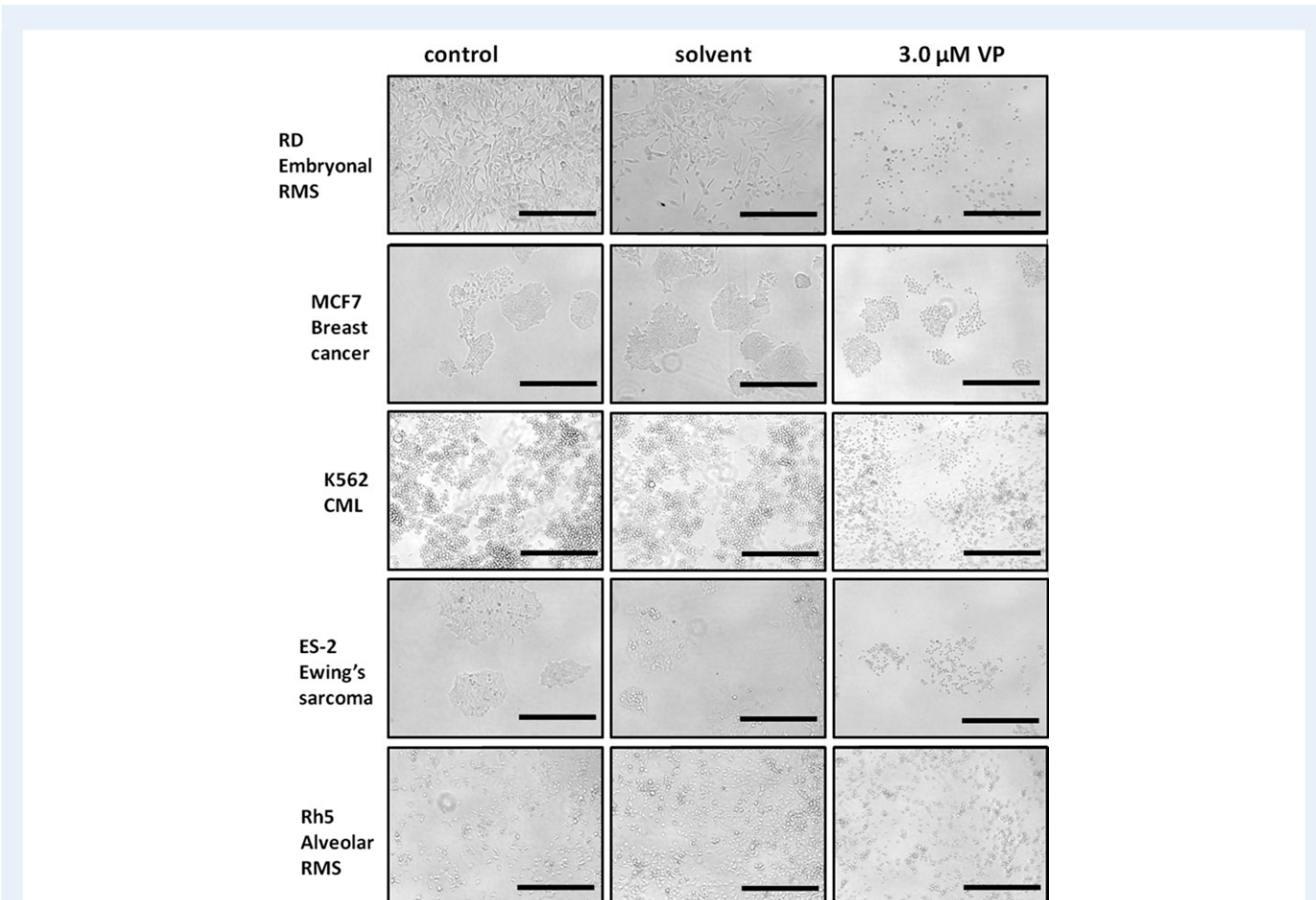


Figure 1 A variety of cancer cell lines are sensitive to Verteporfin (VP) *in vitro*. Human cancer cell lines representing embryonal rhabdomyosarcoma [RD], alveolar rhabdomyosarcoma [Rh5], Ewing's sarcoma [ES-2], breast cancer [MCF7] and chronic myeloid leukaemia [K562] were exposed for 24 h to 3 μ M VP or solvent. All cell lines displayed the morphological features of cell death (e.g. rounding up and detachment, disintegration, membrane blebbing) when exposed to VP, whereas exposure to solvent only had no visible effects on cell morphology. Scale bars represent 400 μ m.

The small molecule Verteporfin (Visudyne, VP) has been shown to directly inhibit the YAP/TAZ oncoproteins (Liu-Chittenden *et al.*, 2012; Wang *et al.*, 2016; Kandoussi *et al.*, 2017), resulting in a specific inhibition of the Hippo pathway downstream. Many cancer types have recently been reported to be sensitive to VP (Brodowska *et al.*, 2014; Feng *et al.*, 2016; Fullenkamp *et al.*, 2016; Al-Moujahed *et al.*, 2017; Kang *et al.*, 2017; Wei *et al.*, 2017). These observations indicate that VP might be an ideal candidate to eradicate malignant cells from human ovarian cortex fragments by *ex vivo* purging.

To study the effect of VP on cancerous cells in ovarian tissue fragments, an *ex vivo* culture method was used based on experimentally induced tumours by micro-injection of various cancer cell lines in ovarian tissue (Peek *et al.*, 2015). Hence, growing tumour foci are efficiently embedded in the ovarian cortex, thereby mimicking actual metastases in the correct physiological environment including the appropriate extracellular matrix (ECM) stiffness. The microenvironment, and especially the stiffness of the ECM, is known to significantly affect the chemo sensitivity of cancer cells (Schrader *et al.*, 2011; Shin and Mooney, 2016; Lin *et al.*, 2017), making this *ex vivo* culture system

the method of choice when testing purging protocols for ovarian cortex tissue.

The main goal of the current study is to design an *ex vivo* treatment using the specific YAP/TAZ inhibitor VP to purge ovarian cortex tissue of malignant cells without compromising ovarian tissue or follicular integrity. This may provide a feasible therapeutic strategy in preventing reintroduction of malignancy due to autotransplantation of ovarian tissue, thereby enhancing the safety of OCT.

Materials and Methods

Collection of material

Human ovarian tissue was collected after informed consent from female-to-male transgender individuals undergoing oophorectomy (eight patients, ages ranging from 19 to 26 years). Whole ovaries were transported on ice in L-15 medium (Lonza, Switzerland) and cortical fragments were prepared and cryopreserved within 4 h after surgery, according to clinical standards (Peek *et al.*, 2015).

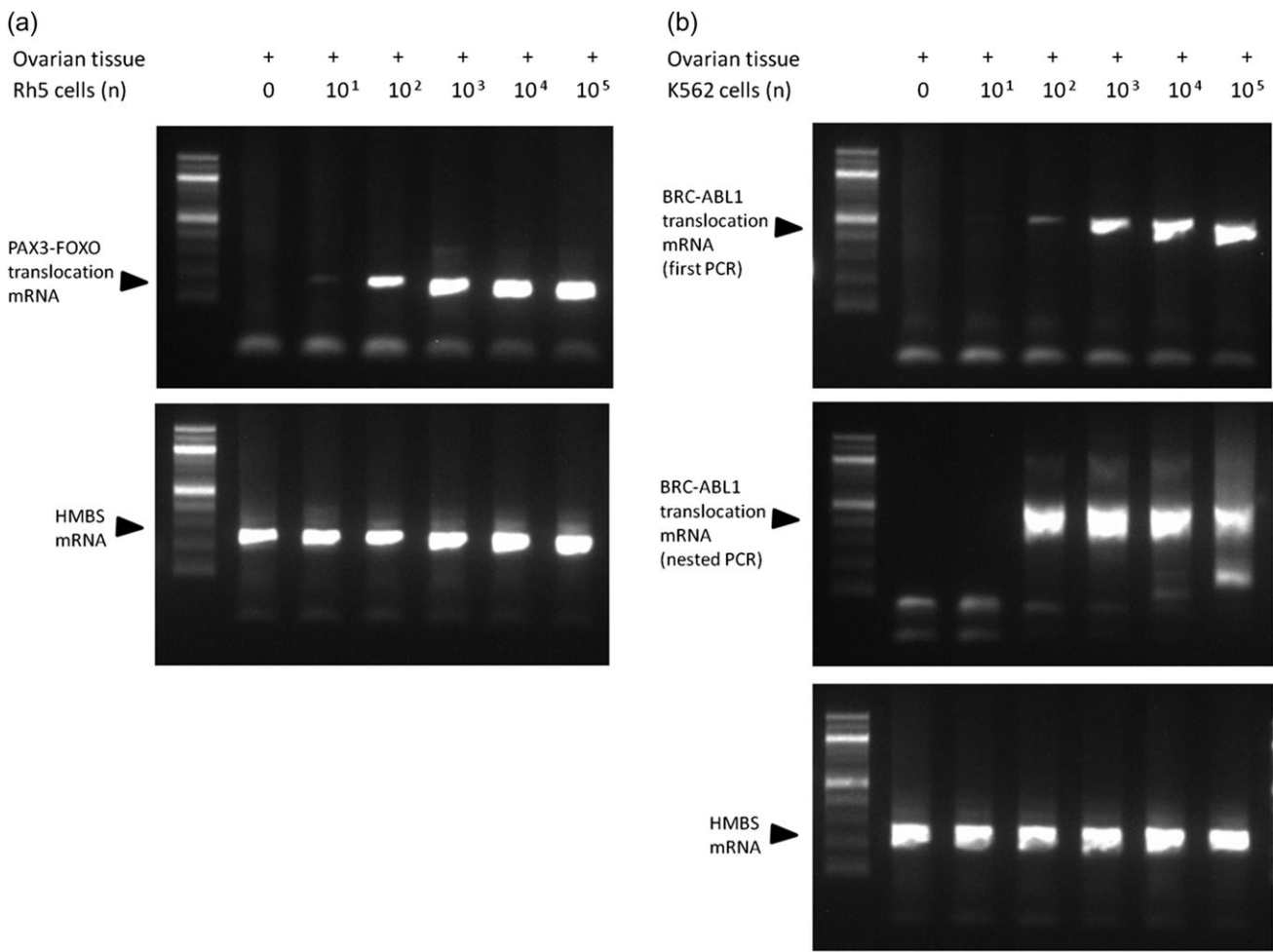


Figure 2 Sensitivity of RT-PCR for the tumour specific translocations. Human ovarian cortex tissue was spiked with increasing numbers of alveolar rhabdomyosarcoma Rh5 cells or chronic myeloid leukaemia K562 cells after which total RNA was isolated and converted to cDNA according to diagnostic standards. (a) The PAX3-FOXO1 transcript was clearly detectable after adding 10 Rh5 cells to ovarian cortex tissue. Taking into account the absolute amount of RNA used for cDNA conversion (1/5th of the total RNA sample) and the input for the PCR (1/20th of the cDNA sample) we reasoned that the detection threshold must be below a single Rh5 cell. (b) The BCR-ABL1 transcript was clearly detectable after adding 100 K562 cells to ovarian cortex tissue after both the first and nested PCR. Even though the nested PCR did not result in a lower detection threshold, the visible signal increased significantly after the nested PCR. Taking into account the absolute amount of RNA used for cDNA conversion (1/5th of the total RNA sample) and the input for the PCR (1/20th of the cDNA sample) we reasoned that the detection threshold must be approximately one K562 cell.

Tumour induction assay and ex vivo purging

To initiate tumour formation in ovarian cortex, cryopreserved ovarian cortex fragments were thawed and micro-injected with freshly cultured cancer cell lines (embryonal rhabdomyosarcoma [RD and Rh36], alveolar rhabdomyosarcoma [Rh5], Ewing's sarcoma [ES-2], breast cancer [MCF7] and chronic myeloid leukaemia [K562]) using forceps and a needle with a 0.4 mm outer diameter as described previously (Peek *et al.*, 2015). Cell lines were originally obtained from ATCC (USA), except for the rhabdomyosarcoma cell lines, who were a gift from Dr Peter Houghton of the Pediatric Preclinical Testing Program (Columbus, OH). Subsequently, the ovarian fragments containing tumours were cultured between 3 and 5 days to allow tumour foci to develop. Fragments were cut into 5×10 mm

pieces and distributed at random over the different treatment groups. The purging treatment was defined as 24 h incubation in 5 ml DMEM supplemented with 10%FCS (including appropriate antibiotics) containing VP (Sigma-Aldrich, Germany) alone, or in combination with Imatinib (Selleckchem, USA) in a six well plate. A control with an equivalent concentration of the VP solvent (dimethyl sulphoxide, DMSO) was included in all experiments. Following a 24 h of pharmacological treatment the fragments were washed using DMEM in clean six wells plates in four consecutive washes at 37°C for 10 min while shaking intermittently to allow optimal diffusion. Cortex fragments were subsequently cultured for 6 additional days to allow for remaining cancer cells to establish new tumour foci. Sufficient tumour formation throughout culture was determined by

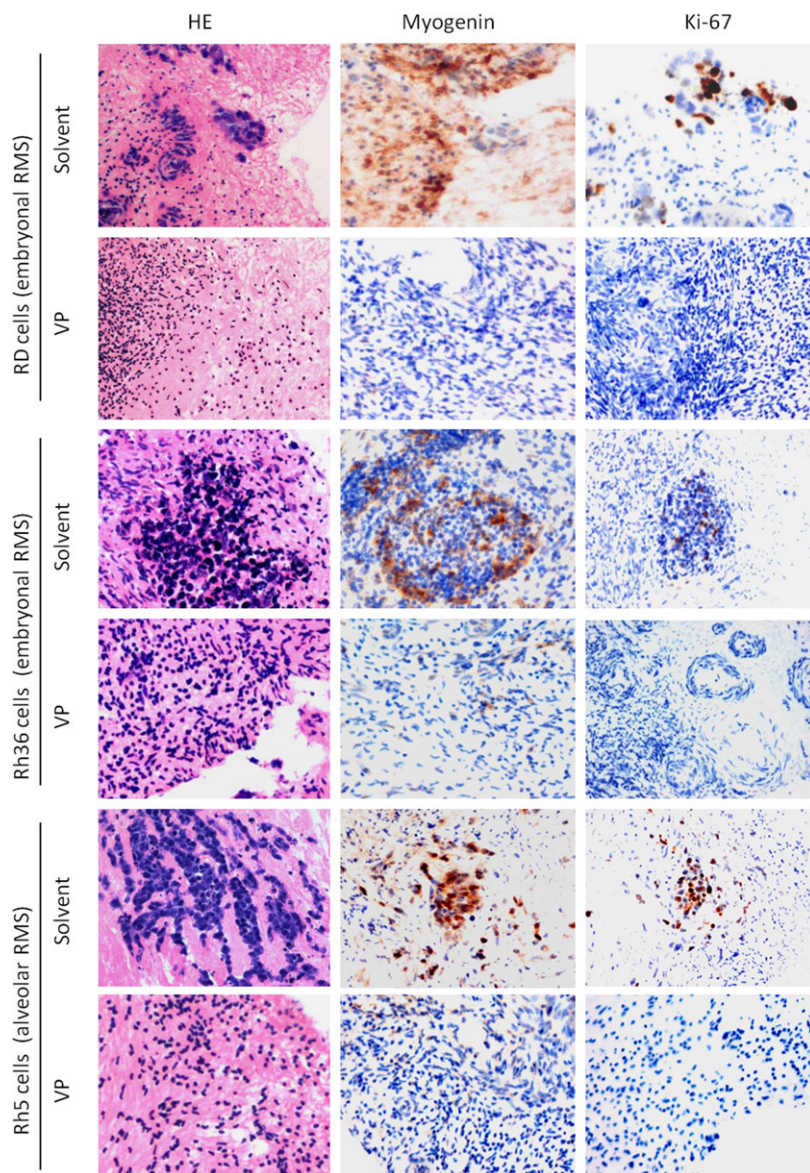


Figure 3 Rhabdomyosarcoma cell lines are sensitive to Verteporfin (VP) in an ovarian cortex culture system. Standard haematoxylin and eosin (HE) shows that RD and Rh36 tumour foci (embryonal phenotype) and Rh5 (alveolar phenotype) were abundant in human ovarian cortex tissue containing RD, Rh36 or Rh5 cells when treated with solvent-only, while no tumour foci could be identified in tissue 6 days after treatment with 3 μ M VP. HE staining was performed on serial sections throughout entire tissue fragments from three patients. Myogenin and Ki-67 immunohistochemical staining was apparent in tissue exposed to solvent-only. Even though myogenin showed marginal background staining in VP treated tissue, proliferating cells could not be detected by immunohistochemical staining for the proliferation marker Ki-67. RMS, rhabdomyosarcoma.

histology. Each experiment was performed in ovarian tissue derived from at least three patients.

Viability assessment of ovarian tissue and follicles

We ascertained viability of ovarian tissue and follicles by three independent methods in tissue of three patients. To assess the viability of the ovarian tissue fragments we measured *in vitro* glucose uptake over a period of 5 days as described previously (Gerritse et al., 2011; Peters

et al., 2017; Westphal et al., 2017). In brief, ovarian tissue fragments (1 \times 1 mm) were cultured in DMEM medium supplemented with 10% FCS and 40 μ g/ml gentamycin. After a culture period of 5 days glucose content in the spent medium was measured to determine the glucose uptake per mg of ovarian tissue. To determine the integrity of the follicles, we evaluated at least 100 primordial and primary follicles (designated as small follicles) in HE stained sections (7 μ m) per condition and per patient after ex vivo purging treatment followed by an additional 24 h culture period to allow potential damage to the follicles to become apparent. We marked follicles as damaged based on the

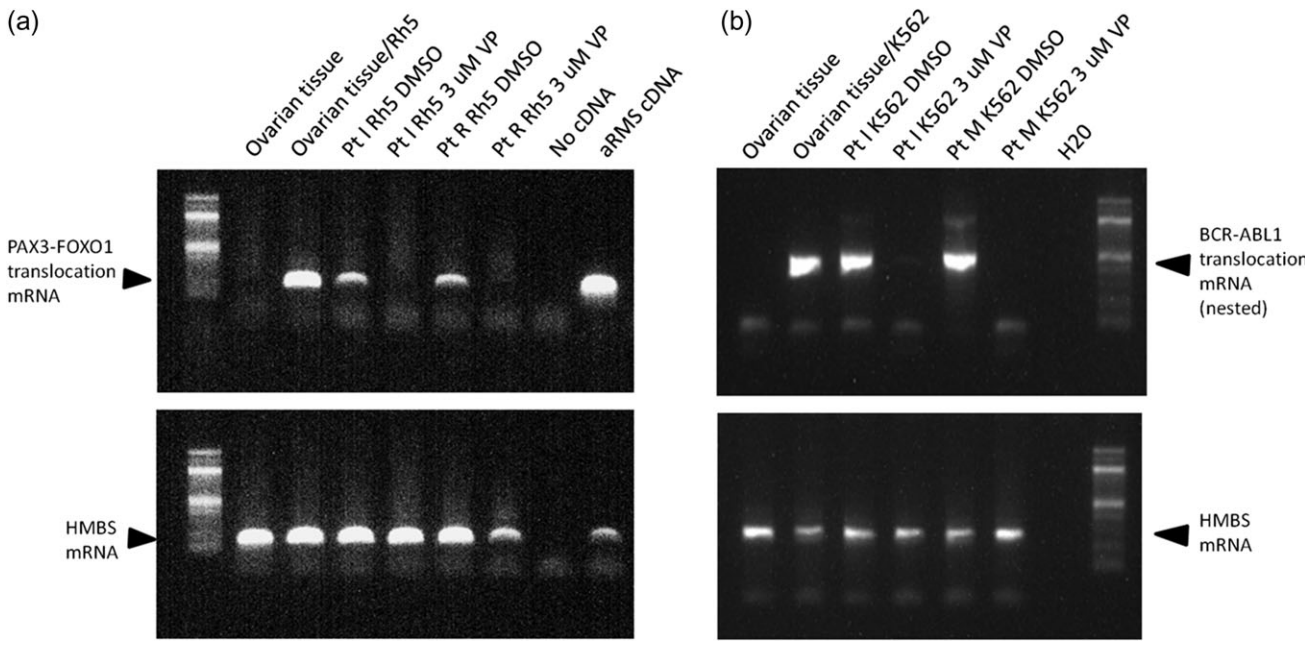


Figure 4 Detection of tumour specific transcripts by RT-PCR. (a) Gel electrophoresis of RT-PCR products of the alveolar rhabdomyosarcoma specific transcript PAX3-FOXO1 performed on cDNA derived from ovarian cortex fragments with proliferating Rh5 cells 6 days after treatment. Ovarian tissue with no malignant cells was used as a negative control while ovarian tissue spiked with Rh5 RMS cells and a tumour sample of alveolar rhabdomyosarcoma served as positive controls. The PAX3-FOXO1 transcript was detected in tissue containing Rh5 tumour foci after treatment with the solvent only (DMSO), but not after treatment with 3 μM of Verteporfin (VP). (b) Gel electrophoresis of nested RT-PCR products of the CML specific transcript BCR-ABL1 performed on cDNA derived from ovarian cortex fragments without cancer cells (negative control) and ovarian tissue with K562 CML cells 6 days after treatment. Ovarian tissue spiked with K562 cells served as a positive control. The BCR-ABL1 transcript was detected in tissue containing K562 tumour foci after treatment with the solvent only (DMSO), but not after treatment with 3 μM VP in patient M. For patient (Pt) I the signal decreased significantly, but a faint signal could be detected in this sample. In A and B expression of the housekeeping gene hydroxymethylbilane synthase (HMBS) was unaffected by VP treatment.

presence of pycnotic oocyte or follicular cell nuclei, contraction of the chromatin of the oocyte, eosine uptake by the oocyte cytoplasm and the detachment or shrinkage of follicular cells (Gougeon, 1986; Keros *et al.*, 2009) after standard Haematoxylin and Eosin (HE) staining (see Histological examination). Finally, the viability of the isolated follicles was studied by Neutral Red uptake (Vanacker *et al.*, 2011; Chiti *et al.*, 2017). In brief, follicles were isolated from treated ovarian cortex tissue by mechanical disruption using tweezers and scalpel after which the tissue was digested in a mixture of Collagenase I (1 mg/ml, Sigma Aldrich, USA), Liberase (2,5 mg/ml, Roche, Switzerland) and DNase I (100 μg/ml, Roche, Switzerland) in DMEM at 37°C for 75 min (Soares *et al.*, 2015). The isolated follicles were pelleted and incubated with McCoy's 5 A medium supplemented with Neutral Red for 90 min at 37°C. The number of Neutral Red positive and negative follicles was counted to calculate the ratio between viable and non-viable follicles.

Histological examination

Tissue was fixated in Bouin's solution (Klinipath, the Netherlands) for 1 h, followed by washing with tap water and storage in ready-to-use 4% formaldehyde solution (Klinipath, the Netherlands) prior to embedding in paraffin. Standard HE staining was performed using an automatic staining machine (Tissue Tek® Prisma™, Sakura, the

Netherlands). For assessment of follicles 7 μm sections were used, while 4 μm sections were used for ovarian cortex containing tumours. To identify tumour foci or cells within tissue fragments containing tumours, HE staining was performed on serial sections throughout the entire fragment (28 μm between sections), after which all sections were evaluated microscopically. To identify malignant cells in (suspected) lesions, an immunohistochemical staining was performed for CD43 for K562 (Lee *et al.*, 2005; Clone DF-T1, DAKO, Agilent Technologies, USA), CD99 for ES-2 (Folpe *et al.*, 2005; Ab-2, clone O13, Neomarkers, USA), Cytokeratin-8 for MCF-7 (Cimpean *et al.*, 2008; Clone CAM 5.2, BD, USA), and Myogenin (Kumar *et al.*, 2000; Clone F5D, Immunologic, the Netherlands) for all rhabdomyosarcoma cell lines. Staining for Ki-67 (Clone MIB-1, DAKO, Agilent Technologies, USA) was used as a proliferation marker and anti active Caspase-3 was used for the detection of apoptosis (Clone C92-605, BD, USA). In brief, after antigen retrieval using tri-sodium citrate dihydrate or EDTA pH 9.0 (Myogenin staining only), sections were incubated with primary antibodies followed by incubation with Biotinylated anti-Mouse (Vector Laboratories, USA). Isotype IgG was included as a negative control. The signal was visualized by incubation with Vectastain AB-complex (Vector Laboratories, USA), followed by incubation with DAB (Vector Laboratories, USA). Haematoxylin was used as counterstaining and slides were evaluated on a Zeiss Axioskop 2

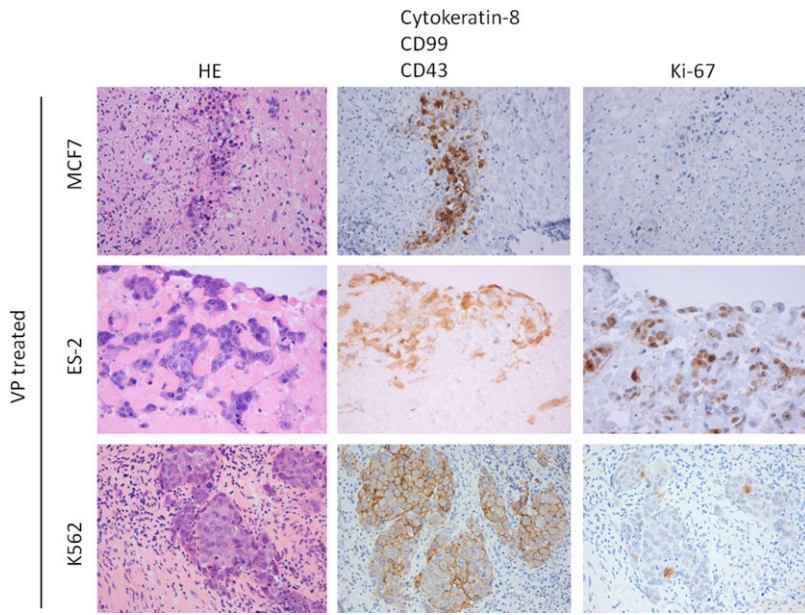


Figure 5 Breast cancer, Ewing's Sarcoma and CML cell lines do not respond to Verteporfin (VP) treatment in an ovarian cortex culture system. Top row: Tumour foci were detectable in human ovarian tissue containing MCF7 breast cancer cells 6 days after treatment with 3.0 μ M VP. Cells within foci were positive for the breast cancer marker cytokeratin-8. Ki-67 immunohistochemical staining was present in a subset of cells, but the signal was weak. Middle row: Viable tumour foci and metastasis in human ovarian tissue containing ES-2 Ewing's sarcoma cells 6 days after treatment with 3.0 μ M VP. Cells expressed the Ewing's sarcoma marker CD99 and cell proliferation was shown by Ki-67 expression. Bottom row: Viable tumour foci were detectable in human ovarian tissue containing K562 CML cells 6 days after treatment with 3.0 μ M VP. Cells within the foci abundantly expressed the CML marker CD43 and some cells were positive for Ki-67.

plus microscope fitted with a Jenoptik ProgRes C10 Plus camera. Images were taken using a 200 \times magnification unless stated otherwise. Tissue sections of human tonsil, pancreas, liver and colon were included as positive controls.

Tumour specific PCR

In addition to (immuno)histochemistry we performed a tumour specific Reverse Transcription- PCR (RT-PCR) to assess whether ovarian cortex fragments containing experimentally induced tumours were sufficiently purged of malignant cells (see Supplementary Materials and Methods). For the alveolar rhabdomyosarcoma specific translocation PAX3-FOXO1 and for the CML specific translocation BCR-ABL1 a nested RT-PCR was performed for the e14a2/e13a2 transcripts (Cross et al., 1994). Both protocols have been validated for diagnostics purposes in our academic hospital.

Results

Verteporfin as a candidate to purge ovarian tissue of various malignancies

To obtain insight into the tumourcidal activity of the YAP/TAZ-inhibitor VP, we first tested the effect of VP on cancer cell lines grown on tissue culture plastic. We investigated the effect of a 24 h treatment of increasing concentrations of VP on a panel of cell lines representing various malignancies. A 24 h treatment using 1.5 μ M VP appeared to

be effective in inducing cell death for RD, Rh5 and ES-2, but not for MCF7 and K562 (results not shown). Exposure to 3.0 μ M VP eradicated all cancer cells effectively within 24 h, whereas incubation with the solvent only had no visible effect on cell morphology (Fig. 1).

Subsequently, we aimed to confirm the tumourcidal activity of a 24 h treatment using 3.0 μ M VP in an ex vivo tumour-induction model (Peek et al., 2015). Briefly, ovarian cortex tissue fragments harbouring tumour foci originating from RD, Rh36, Rh5, ES-2, MCF7 and K562 were exposed to 3.0 μ M VP for 24 h followed by extensive washing to remove the inhibitor. The tissue fragments were cultured for an additional 6 days to allow any remaining cancer cell to form new foci. Evaluation of the tissue fragments was done by immunohistochemistry for tumour specific markers combined with an RT-PCR for a tumour-specific translocation for the alveolar rhabdomyosarcoma Rh5 cells and the chronic myeloid leukaemia K562 cells. The sensitivity of these PCRs was evaluated by spiking ovarian cortex tissue with these cancer cells and revealed a detection level of at least a single cell for both assays (Fig. 2).

Rhabdomyosarcoma cells responded well to VP treatment, as no tumour foci nor proliferating tumour cells could be detected by immunohistochemistry after the ex vivo treatment with 3.0 μ M VP. In the control tissue fragments treated with an equivalent concentration of solvent (DMSO) viable, proliferating tumour foci were abundant at Day 7 (Fig. 3). Efficient purging of the ovarian tissue could be confirmed by the absence of the alveolar rhabdomyosarcoma specific PAX3-FOXO1 translocation transcript in tissue containing experimentally induced Rh5 tumours treated with 3.0 μ M VP (Fig. 4a).

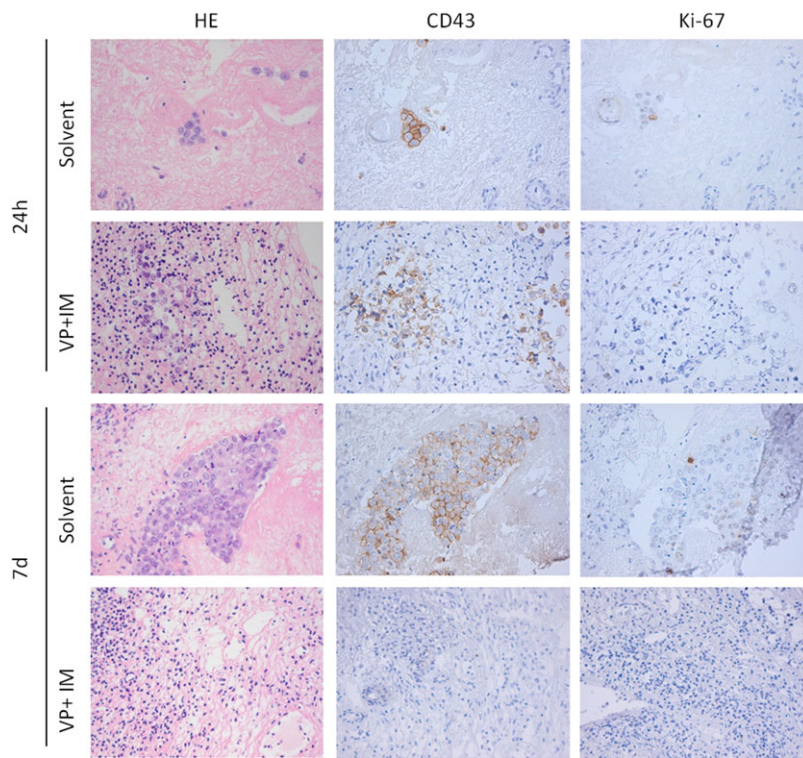


Figure 6 CML cells embedded in ovarian cortex are eradicated by combination treatment with Imatinib (IM) and Verteporfin (VP). Top rows: Human ovarian cortex tissue containing K562 cells was harvested directly after a 24 h treatment using combination treatment (80 μ M IM and 3.0 μ M VP) or solvent only (DMSO). In the solvent only treated fragments small CD43+ foci could be detected harbouring Ki-67 positive cells. In the fragments exposed to the combination therapy tumour foci were disintegrating and cells display characteristics of apoptosis. Ki-67 protein expression was absent within these cells. Bottom rows: Ovarian cortex tissue containing K562 cells was harvested on Day 7 (6 days after treatment) using combination therapy (80 μ M IM and 3.0 μ M VP) or solvent only (DMSO). HE staining was performed on serial sections throughout entire tissue fragment originating from three patients. Large CD43+ viable foci containing dividing cells were present in solvent only treated fragments, while tumour foci were completely absent in fragments exposed to the combination treatment.

While rhabdomyosarcoma cells could effectively be eradicated by a 24 h *ex vivo* treatment using 3.0 μ M VP, breast cancer cell line MCF7, Ewing sarcoma cell line ES-2 and CML cell line K562 appeared to be less affected by this treatment (Fig. 5). In treated ovarian cortex tissue inoculated with MCF7 cells, cells expressing the breast cancer marker cytokeratin-8 could be detected 6 days after treatment with VP. These cells, although morphologically intact were found to only marginally express the proliferation marker Ki-67. Tissue with ES-2 and K562 tumours treated with 3 μ M VP contained numerous viable tumour foci 6 days after treatment, as shown by HE staining and immunostaining for the tumour specific markers CD99 and CD43, and Ki-67, strongly suggesting that these cell types were not sensitive to *ex vivo* VP treatment.

We reasoned that a combination treatment might be more effective in purging ovarian tissue from cancer cells that were not affected by VP treatment only. It was previously shown that VP enhanced the efficacy of the BCR-ABL1 inhibitor Imatinib (IM) in K562 cells (Li *et al.*, 2016). Therefore, we opted for a 24 h *ex vivo* treatment of ovarian cortex fragments harbouring K562 foci using 3.0 μ M VP in combination with 80.0 μ M IM. Directly after treatment, K562 tumour foci were visibly affected (Fig. 6). More importantly, K562 tumour foci could not be

detected by HE staining or immunohistochemistry for the CML specific marker CD43 in VP + IM treated tissue at Day 7 after treatment. We verified the efficacy of the combination treatment by a nested RT-PCR for the CML specific transcript BCR-ABL1, which showed a substantial decrease of this transcript 6 days after *ex vivo* treatment using the 3.0 μ M VP in combination with 80 μ M IM (Fig. 4b).

Verteporfin does not impair ovarian tissue or follicular integrity

To confirm the functional integrity of ovarian cortex fragments treated with VP we investigated the effect of a 24 h *ex vivo* treatment on cortical tissue integrity. We used four independent methods to evaluate the viability of the tissue and the survival and morphology of the small follicles. This was done in separate experiments where ovarian cortex tissue was only exposed to the 24 h VP treatment to mimic future clinical application. Metabolic activity of the ovarian stromal tissue after treatment was not affected by VP as shown by a glucose uptake that was similar compared to tissue exposed to solvent only (Fig. 7). Although glucose uptake was variable between patients, no statistically significant difference could be observed between the conditions.

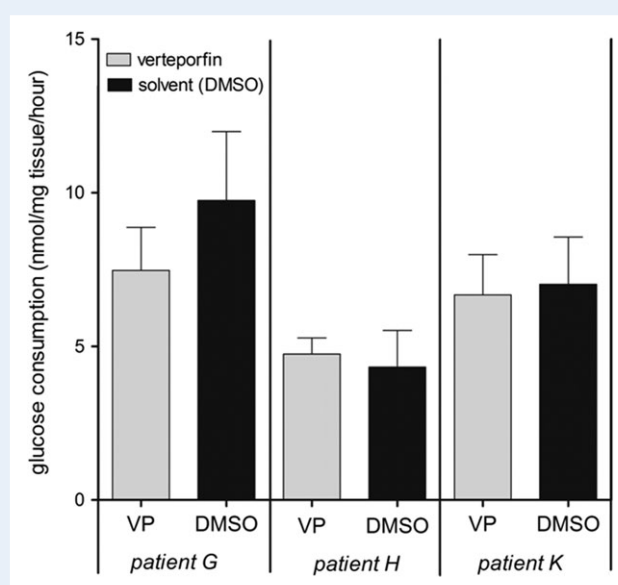


Figure 7 *In vitro* glucose uptake of ovarian cortex treated with Verteporfin (VP) for 24 h. Glucose uptake of ovarian cortex fragments was measured following a 24 h *ex vivo* treatment with 3.0 μ M VP or solvent (DMSO) only. This experiment was performed in four replicates per patient and condition. Error bars stand for standard deviations. No statistically significant differences could be observed in glucose uptake between VP treated and solvent treated tissues ($P > 0.05$).

Moreover, similar percentages of morphologically intact primordial and primary follicles could be identified in treated and control ovarian cortex fragments (Fig. 8a and b). Besides this, we could confirm that this treatment did not reduce the proportion of viable follicles by Neutral red uptake (Fig. 8c and d), since only a 1–7% difference in number of viable follicles can be observed between VP treated and control tissue. Also immunohistochemical staining for the apoptosis marker active Caspase-3 showed no significant difference between VP treated and control tissue (Fig. 8e and f). These results strongly suggest that the 24 h *ex vivo* treatment does not affect ovarian tissue integrity.

Discussion

In this study, we provide for the first time, proof-of-principle that effectively purging ovarian cortex tissue of malignant cells is possible without compromising follicular integrity using a 24 h *ex vivo* pharmacological inhibition of YAP/TAZ oncoproteins by VP. We have shown that it is feasible to effectively remove metastasized rhabdomyosarcoma cells using low concentrations of VP. Moreover, we were able to adapt this treatment for CML by combining VP with IM. Importantly, a 24 h treatment with VP did not negatively affect ovarian stromal metabolism, follicular morphology or follicular viability.

Using a previously established tumour induction model (Peek et al., 2015) based on micro-injection of cancer cells into human ovarian cortex tissue, we were able to efficiently create proliferating, metastasis-like tumour foci in the ovarian tissue in a unique organ culture system. Since human ovarian cortex tissue from cancer patients available for

research purposes is scarce, we resided to ovarian tissue from transgender patients undergoing female-to-male transition. Ovarian tissue from these patients is considered a suitable source for research because of the normal morphology of the tissue (Caanen et al., 2017; De Roo et al., 2017). In this model we opted for cancer cell lines rather than primary cancer cells. Even though cell lines may not fully mirror the biology of primary cancer cells, their long-term proliferation potential *in vitro* allowed us to perform the required culture experiments which would have been challenging, if not impossible, using primary cancer cells. Moreover, given that the majority of oncogenic alterations are present in cancer cell lines, cell lines are indeed considered to be a valuable model in anti-cancer drug screening (Iorio et al., 2016). All in all, this model allowed us to analyse the effect of the inhibitors on the cancer cells in the appropriate microenvironment (Bastings et al., 2013; Peek et al., 2015).

The cancer cell microenvironment is crucial for testing the effect of pharmacological eradication of tumours and by using this organ culture system, we could test VP on proliferating cancer cells in a tumour microenvironment with ECM components and rigidity that are identical to the *in vivo* situation. In general, incorporation of components of the microenvironment is considered to be beneficial in high throughput drug discovery (Lovitt et al., 2014). Specifically, the rigidity of the ECM has shown to have a strong influence on the expression of the VP targets YAP/TAZ (Lin et al., 2017). Moreover, high ECM stiffness (as in ovarian cortex) induced nuclear localization of YAP and TAZ, leading to high transcriptional activity of downstream effectors (Dupont et al., 2011). Besides this, YAP and TAZ are known to mediate and sense ECM stiffness (Dupont et al., 2011; Calvo et al., 2013). The importance of assessing the effect of VP on various malignancies in the ovarian microenvironment is illustrated in this study by our observation that MCF7, ES-2 and K562 cell lines grown on plastic were effectively ablated by 24 h incubation with VP in a simple *in vitro* test, while these cell lines were largely resistant to this treatment in our *ex vivo* model. This discrepancy provides indirect evidence that microenvironment including ECM stiffness plays a major role in sensitivity to YAP/TAZ-inhibitors and justifies our model system to develop purging protocols in which the cancer cells are in direct contact with the ovarian cortex ECM.

By investigating the tissue extensively using a combination of (immuno)histochemistry and RT-PCR we surpassed the standard clinical pathological examination (often involving evaluation of a few tissue sections) which is routinely performed by a local pathologist prior to transplantation of the ovarian tissue. In this study, we examined the entire tissue fragment by serial sectioning to ensure no tumour foci were present in the treated tissue fragments. To confirm these results, we utilized a sensitive tumour-specific RT-PCR assay, capable of detecting a single malignant cell in the context of the ovarian cortex tissue. By doing so, we were able to show that a 24 h treatment with 3.0 μ M VP is effective in eliminating both alveolar and embryonal rhabdomyosarcoma cells from the ovarian tissue, a concentration which is in the range of previously published studies on the anti-tumour properties of VP (Liu-Chittenden et al., 2012; Feng et al., 2016). The combined action of VP and IM was required to purge the tissue of CML, which is in line with the synergistic effect of these compounds that was previously described for CML cells (Li et al., 2016). After treatment with the VP and IM, no tumour foci could be identified by (immuno)histochemistry. Also, a significant reduction of the CML-specific transcript BCR-ABL1 could be

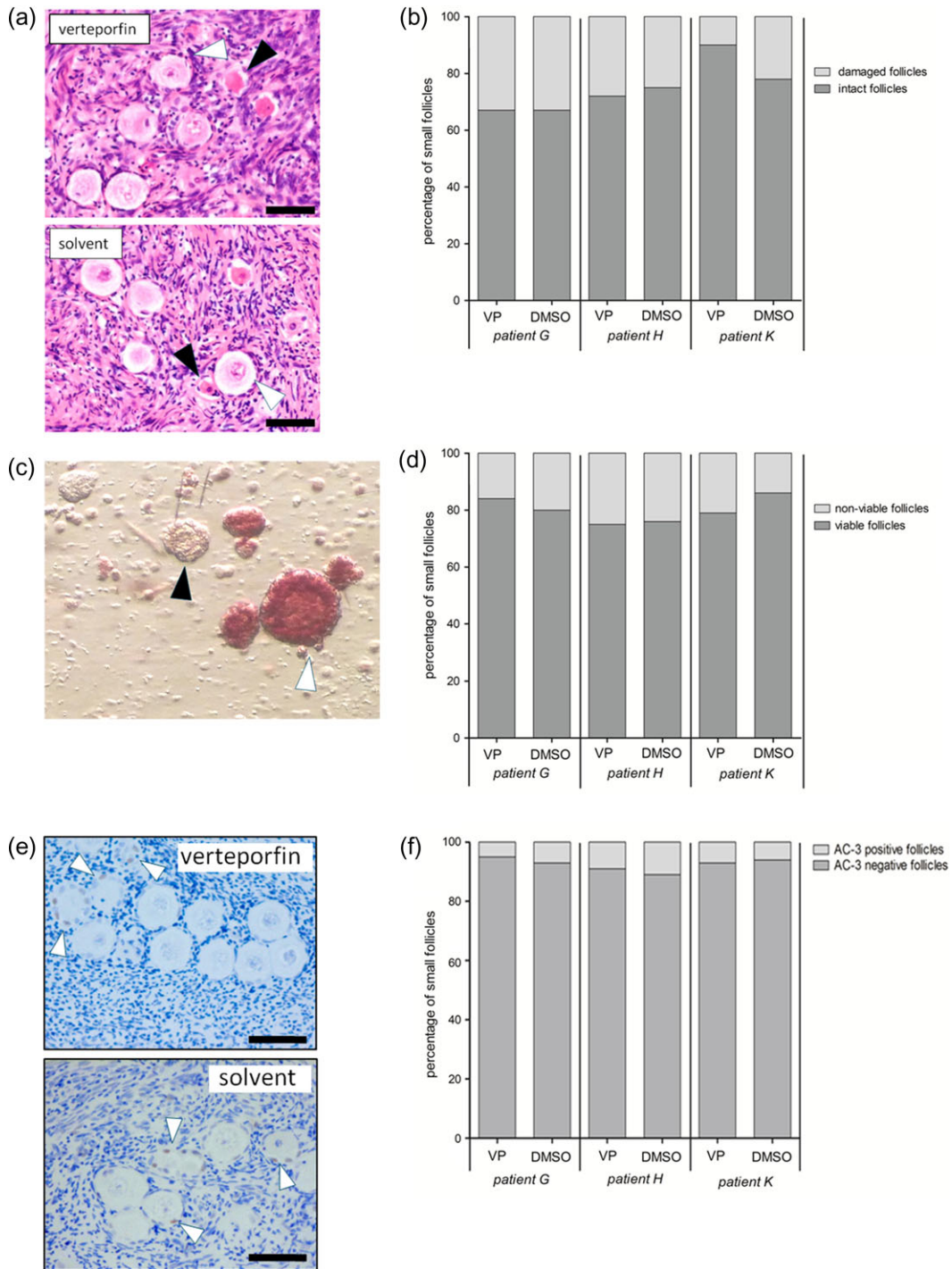


Figure 8 Follicle morphology and viability after 24 h Verteporfin (VP) treatment of ovarian cortex tissue. Ovarian cortex tissue was exposed to a 24 h ex vivo treatment with 3.0 μ M VP or solvent (DMSO) only. **(a)** Representative images of histology of the ovarian cortex after exposure to VP or solvent. Tissue fragments were exposed to an additional 24 h culture to allow potential damage to the follicles to become apparent. White arrowheads: examples of intact primordial follicles. Black arrowheads: examples of damaged primordial follicles. **(b)** Graphical depiction of the percentage of intact and damaged small follicles (primary and primordial) per patient and condition. At least 100 follicles were evaluated per sample. **(c)** Representative image of the Neutral red staining performed on isolated follicles. White arrowhead points to a viable Neutral red positive follicle. Black arrowhead points to a non-viable Neutral red negative follicle. **(d)** Graphical depiction of the percentage of viable and non-viable follicles based on Neutral red staining. At least 100 follicles were evaluated per sample. **(e)** Detection of apoptosis in small follicles by immunohistochemical staining for active Caspase-3. Some follicles showed positive staining of one or more granulosa cells (white arrow heads) but no staining of oocytes was observed. **(f)** Graphical depiction of the percentage of follicles with active Caspase-3 positive granulosa cells. At least 50 follicles were evaluated per sample.

identified by RT-PCR. In one sample, a weak band could be identified in a VP treated sample. The half life of the BCR-ABL1 transcript is considered to be relatively long (~8 h) (Collins et al., 1987). In combination with the absence of perfusion during organ culture residual BCR-ABL1 mRNA may linger in the ovarian tissue fragments after purging, explaining the weak positive result in one patient sample.

Besides the effectiveness of the purging treatment against malignant cells, the functional integrity of the ovarian cortex tissue needs to be safeguarded to maximize the chances of a successful pregnancy in these patients after OCT. Therefore an ex vivo purging protocol that does not harm small follicles and their surrounding ovarian stromal cell compartment is crucial. In our study we found no detrimental effects of a 24 h VP treatment on *in vitro* glucose uptake of the ovarian tissue, viability of small follicles directly after treatment, on the morphology of the small follicles or the percentage of follicles with apoptotic cells. This indicates that our ex vivo purging procedure may not impair ovarian cortex tissue function. For treating CML, we opted for the synergistic action of VP and IM (Li et al., 2016). It was previously established in animal models that IM does not affect female fertility (Administration, 2006; Schultheis et al., 2012). One case study described diminished fertility in a woman after on IM treatment (400–800 mg/per day for 2 years) (Christopoulos et al., 2008). However, given the fact that we used low dosages (80 mg/L medium) for only 24 h, we assumed no detrimental effect on the follicular or ovarian integrity of the combination treatment.

By opting for a 24 h ex vivo treatment we adhere to the notion that ex vivo culture of ovarian tissue is preferably short, since culture of ovarian cortex been associated with activation of pre-antral follicles (McLaughlin et al., 2014), which is undesirable because of the risk of follicular burn-out after transplantation (Gavish et al., 2014). A two-day ex vivo treatment of ovarian tissue has previously resulted in a live birth, and therefore short ex vivo culture may not be detrimental to the functional integrity of the tissue. Interestingly, in ovarian tissue from POI patients ex vivo disruption of the Hippo pathway in ovarian tissue fragments promoted follicle stimulation in ovarian tissue, while VP inhibited fragmentation-induced growth in ovarian tissue fragments (Kawamura et al., 2013). This suggests that VP may be a double-edged sword efficiently eradicating malignant cells, while simultaneously preventing culture-induced follicular burn-out and hence integrity of the ovarian tissue.

Even though our results are hopeful in the light of functionality of the ovarian tissue after transplantation, we were not able to test the functionality of the oocytes (i.e. capacity of being fertilized) due to technical difficulties and restrictions by law.

When designing treatment involving gametes for the purpose of reproduction, one needs to take into account the potential risks for the offspring that will be derived from these gametes. Even though ex vivo culture of ovarian cortex tissue preceding autotransplantation has been performed before and resulted in live birth in human (Kawamura et al., 2013), too few children have been born to draw conclusions on the safety of ex vivo ovarian tissue culture in combination with OCT. In this study we exposed ovarian cortex to VP, which is an approved FDA category C drug. This FDA category implies that even though administration of high dosages of VP throughout pregnancy in animal models resulted in an increased risk of developmental disorders to the eye, usage of VP in pregnant women is allowed if benefits for the woman outweigh the potential risks. In humans, only few cases of VP exposure during pregnancy have been reported with

no adverse effects to the foetus (De Santis et al., 2004; Rodrigues et al., 2009; Rosen et al., 2009). Considering IM, natural conception and uneventful pregnancies in women using IM have been reported (Ault et al., 2006; Zhou et al., 2013). Even though both VP and IM appear to be a low risk agents, systematic studies towards the possible risks of ex vivo culture of ovarian cortex and follicular VP exposure for the offspring are needed (Harper et al., 2012; Mulder et al., 2018; Sharpe, 2018).

Despite these reservations, the results in this paper indicate that effective purging of ovarian cortex tissue intended for fertility preservation purposes from cancer cells of solid tumours or leukaemia is possible by short-term ex vivo treatment using specific YAP/TAZ inhibitors. Hereby we provide a feasible therapeutic strategy in preventing reintroduction of malignancy due to autotransplantation of ovarian tissue. This increases the likelihood that this form of fertility restoration may become an option for patients with malignancies for which OCT is currently considered unsafe.

Supplementary data

Supplementary data are available at *Human Reproduction* online.

Acknowledgements

We would like to thank Marian Verdijk for her assistance with the RT-PCRs and Bert van der Reijden for providing us the relevant primer sets and protocol for the BCR-ABL1 RT-PCR.

Authors' roles

The project and experiments were designed by R.P., C.L.M., D.D.M.B. and C.C.M.B. Experiments were performed by C.L.M., L.L.E., and R.P. C.L.M. drafted the original manuscript. All authors critically reviewed and revised the manuscript and approved the final version.

Funding

Unconditional funding was received from Merck B.V. (The Netherlands), an affiliate of Merck KGaA, Darmstadt, Germany (Number 2016-FERT-1) and the foundation 'Radboud Oncologie Fonds' (Number KUN 00007682).

Conflict of interest

The authors report no financial or other conflict of interest relevant to the subject of this article.

References

- Administration FaD. Revised Product Label Gleevec (Imatinib Mesylate). 2006.
- Ahmed AA, Abedalthagafi M, Anwar AE, Bui MM. Akt and Hippo pathways in Ewing's sarcoma tumors and their prognostic significance. *J Cancer* 2015;6:1005–1010.
- Al-Moujahed A, Brodowska K, Stryjewski TP, Efthathiou NE, Vasilikos I, Cichy J, Miller JW, Gragoudas E, Vavvas DG. Verteporfin inhibits growth of human glioma *in vitro* without light activation. *Sci Rep* 2017;7:7602.

Ault P, Kantarjian H, O'Brien S, Faderl S, Beran M, Rios MB, Koller C, Giles F, Keating M, Talpaz M et al. Pregnancy among patients with chronic myeloid leukemia treated with imatinib. *J Clin Oncol* 2006; **24**: 1204–1208.

Azem F, Hasson J, Ben-Yosef D, Kossoy N, Cohen T, Almog B, Amit A, Lessing JB, Lifschitz-Mercer B. Histologic evaluation of fresh human ovarian tissue before cryopreservation. *Int J Gynecol Pathol* 2010; **29**: 19–23.

Bartee E, Chan WM, Moreb JS, Cogle CR, McFadden G. Selective purging of human multiple myeloma cells from autologous stem cell transplantation grafts using oncolytic myxoma virus. *Biol Blood Marrow Transplant* 2012; **18**: 1540–1551.

Bartucci M, Dattilo R, Moriconi C, Pagliuca A, Mottolese M, Federici G, Benedetto AD, Todaro M, Stassi G, Sperati F et al. TAZ is required for metastatic activity and chemoresistance of breast cancer stem cells. *Oncogene* 2015; **34**: 681–690.

Bastings L, Beerendonk CC, Westphal JR, Massuger LF, Kaal SE, van Leeuwen FE, Braat DD, Peek R. Autotransplantation of cryopreserved ovarian tissue in cancer survivors and the risk of reintroducing malignancy: a systematic review. *Hum Reprod Update* 2013; **19**: 483–506.

Brodowska K, Al-Moujahed A, Marmalidou A, Meyer Zu Horste M, Cichy J, Miller JW, Gragoudas E, Vavas DG. The clinically used photosensitizer Verteporfin (VP) inhibits YAP-TEAD and human retinoblastoma cell growth in vitro without light activation. *Exp Eye Res* 2014; **124**: 67–73.

Caanen MR, Schouten NE, Kuijper EAM, van Rijswijk J, van den Berg MH, van Dulmen-den Broeder E, Overbeek A, van Leeuwen FE, van Trotsenburg M, Lambalk CB. Effects of long-term exogenous testosterone administration on ovarian morphology, determined by transvaginal (3D) ultrasound in female-to-male transsexuals. *Hum Reprod* 2017; **32**: 1457–1464.

Calvo F, Ege N, Grande-Garcia A, Hooper S, Jenkins RP, Chaudhry SI, Harrington K, Williamson P, Moeendarbary E, Charras G et al. Mechanotransduction and YAP-dependent matrix remodelling is required for the generation and maintenance of cancer-associated fibroblasts. *Nat Cell Biol* 2013; **15**: 637–646.

Chiti MC, Dolmans MM, Hobeika M, Cernogoraz A, Donnez J, Amorim CA. A modified and tailored human follicle isolation procedure improves follicle recovery and survival. *J Ovarian Res* 2017; **10**: 71.

Chiti MC, Dolmans MM, Mortiaux L, Zhuge F, Ouni E, Shahri PAK, Van Ruymbeke E, Champagne SD, Donnez J, Amorim CA. A novel fibrin-based artificial ovary prototype resembling human ovarian tissue in terms of architecture and rigidity. *J Assist Reprod Genet* 2018; **35**: 41–48.

Christopoulos C, Dimakopoulou V, Rotas E. Primary ovarian insufficiency associated with imatinib therapy. *N Engl J Med* 2008; **358**: 1079–1080.

Collins S, Coleman H, Groudine M. Expression of bcr and bcr-abl fusion transcripts in normal and leukemic cells. *Mol Cell Biol* 1987; **7**: 2870–2876.

Cross NC, Melo JV, Feng L, Goldman JM. An optimized multiplex polymerase chain reaction (PCR) for detection of BCR-ABL fusion mRNAs in haematological disorders. *Leukemia* 1994; **8**: 186–189.

Cîmpean AM, Suciu C, Ceaușu R, Tătăcu D, Mureșan AM, Raica M. Relevance of the immunohistochemical expression of cytokeratin 8/18 for the diagnosis and classification of breast cancer. *Rom J Morphol Embryol* 2008; **49**: 479–483.

De Roo C, Lierman S, Tillemans K, Peynshaert K, Braeckmans K, Caanen M, Lambalk CB, Weyers S, T'Sjoen G, Cornelissen R et al. Ovarian tissue cryopreservation in female-to-male transgender people: insights into ovarian histology and physiology after prolonged androgen treatment. *Reprod Biomed Online* 2017; **34**: 557–566.

De Santis M, Carducci B, De Santis L, Lucchese A, Straface G. First case of post-conception Verteporfin exposure: pregnancy and neonatal outcome. *Acta Ophthalmol Scand* 2004; **82**: 623–624.

Dolmans MM. Recent advances in fertility preservation and counseling for female cancer patients. *Expert Rev Anticancer Ther* 2018; **18**: 115–120.

Dolmans MM, Marinescu C, Saussoy P, Van Langendonck A, Amorim C, Donnez J. Reimplantation of cryopreserved ovarian tissue from patients with acute lymphoblastic leukemia is potentially unsafe. *Blood* 2010; **116**: 2908–2914.

Donnez J, Dolmans MM. Fertility preservation in women. *N Engl J Med* 2017; **377**: 1657–1665.

Donnez J, Dolmans MM, Demly D, Jadoul P, Pirard C, Squifflet J, Martinez-Madrid B, van Langendonck A. Livebirth after orthotopic transplantation of cryopreserved ovarian tissue. *Lancet* 2004; **364**: 1405–1410.

Dupont S, Morsut L, Aragona M, Enzo E, Giulitti S, Cordenonsi M, Zanconato F, Le Digabel J, Forcato M, Bicciato S et al. Role of YAP/TAZ in mechanotransduction. *Nature* 2011; **474**: 179–183.

Feng J, Gou J, Jia J, Yi T, Cui T, Li Z. Verteporfin, a suppressor of YAP-TEAD complex, presents promising antitumor properties on ovarian cancer. *Onco Targets Ther* 2016; **9**: 5371–5381.

Folpe AL, Goldblum JR, Rubin BP, Shehata BM, Liu W, Dei Tos AP, Weiss SW. Morphologic and immunophenotypic diversity in Ewing family tumors: a study of 66 genetically confirmed cases. *Am J Surg Pathol* 2005; **29**: 1025–1033.

Fullenkamp CA, Hall SL, Jaber OL, Pakalniskis BL, Savage EC, Savage JM, Ofori-Amanfo GK, Lambertz AM, Ivins SD, Stipp CS et al. TAZ and YAP are frequently activated oncproteins in sarcomas. *Oncotarget* 2016; **7**: 30094–30108.

Gavish Z, Peer G, Roness H, Cohen Y, Meirow D. Follicle activation and 'burn-out' contribute to post-transplantation follicle loss in ovarian tissue grafts: the effect of graft thickness. *Hum Reprod* 2014; **29**: 989–996.

Gerritse R, Beerendonk CC, Westphal JR, Bastings L, Braat DD, Peek R. Glucose/lactate metabolism of cryopreserved intact bovine ovaries as a novel quantitative marker to assess tissue cryodamage. *Reprod Biomed Online* 2011; **23**: 755–764.

Gougeon A. Dynamics of follicular growth in the human: a model from preliminary results. *Hum Reprod* 1986; **1**: 81–87.

Harper J, Magli MC, Lundin K, Barratt CL, Brison D. When and how should new technology be introduced into the IVF laboratory? *Hum Reprod* 2012; **27**: 303–313.

Harvey KF, Zhang X, Thomas DM. The Hippo pathway and human cancer. *Nat Rev Cancer* 2013; **13**: 246–257.

Iorio F, Knijnenburg TA, Vis DJ, Bignell GR, Menden MP, Schubert M, Aben N, Goncalves E, Barthorpe S, Lightfoot H et al. A landscape of pharmacogenomic interactions in. *Cancer Cell* 2016; **166**: 740–754.

Jensen AK, Macklon KT, Fedder J, Ernst E, Humaidan P, Andersen CY. 86 Successful births and 9 ongoing pregnancies worldwide in women transplanted with frozen-thawed ovarian tissue: focus on birth and perinatal outcome in 40 of these children. *J Assist Reprod Genet* 2017; **34**: 325–336.

Kandoussi I, Lakhili W, Taoufik J, Ibrahimi A. Docking analysis of verteporfin with YAP WW domain. *Bioinformation* 2017; **31**: 237–240.

Kang MH, Jeong GS, Smoot DT, Ashktorab H, Hwang CM, Kim BS, Kim HS, Park YY. Verteporfin inhibits gastric cancer cell growth by suppressing adhesion molecule FAT1. *Oncotarget* 2017; **8**: 98887–98897.

Kawamura K, Cheng Y, Suzuki N, Deguchi M, Sato Y, Takae S, Ho CH, Kawamura N, Tamura M, Hashimoto S et al. Hippo signaling disruption and Akt stimulation of ovarian follicles for infertility treatment. *Proc Natl Acad Sci U S A* 2013; **110**: 17474–17479.

Keros V, Xella S, Hultenby K, Pettersson K, Sheikhi M, Volpe A, Hreinsson J, Hovatta O. Vitrification versus controlled-rate freezing in cryopreservation of human ovarian tissue. *Hum Reprod* 2009; **24**: 1670–1683.

Kreissman SG, Seeger RC, Matthay KK, London WB, Sparto R, Grupp SA, Haas-Kogan DA, Laquaglia MP, Yu AL, Diller L et al. Purged versus non-purged peripheral blood stem-cell transplantation for high-risk

neuroblastoma (COG A3973): a randomised phase 3 trial. *Lancet Oncol* 2013; **14**:999–1008.

Kumar S, Perlman E, Harris CA, Raffeld M, Tsokos M. Myogenin is a specific marker for rhabdomyosarcoma: an immunohistochemical study in paraffin-embedded tissues. *Mod Pathol* 2000; **13**:988–993.

Lee PS, Beneck D, Weisberger J, Gorczyca W. Coexpression of CD43 by benign B cells in the terminal ileum. *Appl Immunohistochem Mol Morphol* 2005; **13**:138–141.

Leone F, Cavalloni G, Gunetti M, Pignochino Y, Piacibello W, Aglietta M. Tumor cell purging by ex vivo expansion of hemopoietic stem cells from breast cancer patients combined with targeting ErbB receptors. *Biol Blood Marrow Transplant* 2006; **12**:68–74.

Levine J. Gonadotoxicity of cancer therapies in pediatric and reproductive-age females. In: Gracia C, Woodruff TK (eds). *Oncofertility Medical Practice: Clinical Issues and Implementation*. New York, NY: Springer New York, 2012, 3–14.

Li H, Huang Z, Gao M, Huang N, Luo Z, Shen H, Wang X, Wang T, Hu J, Feng W. Inhibition of YAP suppresses CML cell proliferation and enhances efficacy of imatinib in vitro and in vivo. *J Exp Clin Cancer Res* 2016; **35**:134.

Lin CH, Jokela T, Gray J, LaBarge MA. Combinatorial microenvironments impose a continuum of cellular responses to a single pathway-targeted anti-cancer compound. *Cell Rep* 2017; **21**:533–545.

Liu-Chittenden Y, Huang B, Shim JS, Chen Q, Lee SJ, Anders RA, Liu JO, Pan D. Genetic and pharmacological disruption of the TEAD-YAP complex suppresses the oncogenic activity of YAP. *Genes Dev* 2012; **26**:1300–1305.

Lovitt CJ, Shelpet TB, Avery VM. Advanced cell culture techniques for cancer drug discovery. *Biology* 2014; **3**:345–367.

McLaughlin M, Albertini DF, Wallace WHB, Anderson RA, Telfer EE. Metaphase II oocytes from human unilaminar follicles grown in a multi-step culture system. *Mol Hum Reprod* 2018; **24**:135–142.

McLaughlin M, Kinnell HL, Anderson RA, Telfer EE. Inhibition of phosphatase and tensin homologue (PTEN) in human ovary in vitro results in increased activation of primordial follicles but compromises development of growing follicles. *Mol Hum Reprod* 2014; **20**:736–744.

Meirow D, Levron J, Eldar-Geva T, Hardan I, Fridman E, Zalel Y, Schiff E, Dor J. Pregnancy after transplantation of cryopreserved ovarian tissue in a patient with ovarian failure after chemotherapy. *N Engl J Med* 2005; **353**:318–321.

Mulder CL, Serrano JB, Catsburg LAE, Roseboom TJ, Repping S, Van Pelt AMM. A practical blueprint to systematically study life-long health consequences of novel medically assisted reproductive treatments. *Hum Reprod* 2018; **33**:784–792.

Peek R, Basting L, Westphal JR, Massuger LF, Braat DD, Beerendonk CC. A preliminary study on a new model system to evaluate tumour-detection and tumour-purging protocols in ovarian cortex tissue intended for fertility preservation. *Hum Reprod* 2015; **30**:870–876.

Peters IT, van Zwet EW, Smit VT, Liefers GJ, Kuppen PJ, Hilders CG, Trimbos JB. Prevalence and risk factors of ovarian metastases in breast cancer patients < 41 years of age in the Netherlands: a nationwide retrospective cohort study. *PLoS One* 2017; **12**:e0168277.

Rodrigues M, Meira D, Batista S, Carrilho MM. Accidental pregnancy exposure to verteporfin: obstetrical and neonatal outcomes: a case report. *Aust N Z J Obstet Gynaecol* 2009; **49**:236–237.

Rosen E, Rubowitz A, Ferencz JR. Exposure to verteporfin and bevacizumab therapy for choroidal neovascularization secondary to punctate inner choroidopathy during pregnancy. *Eye (Lond)* 2009; **23**:1479.

Rosendahl M, Andersen MT, Ralfkiaer E, Kjeldsen L, Andersen MK, Andersen CY. Evidence of residual disease in cryopreserved ovarian cortex from female patients with leukemia. *Fertil Steril* 2010; **94**:2186–2190.

Schrader J, Gordon-Walker TT, Aucott RL, van Deemter M, Quaas A, Walsh S, Benten D, Forbes SJ, Wells RG, Iredale JP. Matrix stiffness modulates proliferation, chemotherapeutic response, and dormancy in hepatocellular carcinoma cells. *Hepatology* 2011; **53**:1192–1205.

Schroder CP, Timmer-Bosscha H, Wijchman JG, de Leij LF, Hollema H, Heineman MJ, de Vries EG. An in vitro model for purging of tumour cells from ovarian tissue. *Hum Reprod* 2004; **19**:1069–1075.

Schultheis B, Nijmeijer BA, Yin H, Gosden RG, Melo JV. Imatinib mesylate at therapeutic doses has no impact on folliculogenesis or spermatogenesis in a leukaemic mouse model. *Leuk Res* 2012; **36**:271–274.

Schuring AN, Fehm T, Behringer K, Goeckenjan M, Wimberger P, Henes M, Henes J, Fey MF, von Wolff M. Practical recommendations for fertility preservation in women by the FertiPROTEKT network. Part I: indications for fertility preservation. *Arch Gynecol Obstet* 2018; **297**:241–255.

Shapira M, Raanani H, Barshack I, Amariglio N, Derech-Haim S, Marciano MN, Schiff E, Orvieto R, Meirow D. First delivery in a leukemia survivor after transplantation of cryopreserved ovarian tissue, evaluated for leukemia cells contamination. *Fertil Steril* 2018; **109**:48–53.

Sharpe RM. Of mice and men: long-term safety of assisted reproduction treatments. *Hum Reprod* 2018; **33**:793–796.

Shin JW, Mooney DJ. Extracellular matrix stiffness causes systematic variations in proliferation and chemosensitivity in myeloid leukemias. *Proc Natl Acad Sci U S A* 2016; **113**:12126–12131.

Silber SJ, Lenahan KM, Levine DJ, Pineda JA, Gorman KS, Friez MJ, Crawford EC, Gosden RG. Ovarian transplantation between monozygotic twins discordant for premature ovarian failure. *N Engl J Med* 2005; **353**:58–63.

Slemmons KK, Crose LE, Rudzinski E, Bentley RC, Linardic CM. Role of the YAP oncoprotein in priming ras-driven rhabdomyosarcoma. *PLoS One* 2015; **10**:e0140781.

Soares M, Sahrari K, Amorim CA, Saussoy P, Donnez J, Dolmans MM. Evaluation of a human ovarian follicle isolation technique to obtain disease-free follicle suspensions before safely grafting to cancer patients. *Fertil Steril* 2015; **104**:672–680.

Vanacker J, Camboni A, Dath C, Van Langendonck A, Dolmans MM, Donnez J, Amorim CA. Enzymatic isolation of human primordial and primary ovarian follicles with Liberase DH: protocol for application in a clinical setting. *Fertil Steril* 2011; **96**:379–383.e373.

von Wolff M, Germeyer A, Liebenthron J, Korell M, Nawroth F. Practical recommendations for fertility preservation in women by the FertiPROTEKT network. Part II: fertility preservation techniques. *Arch Gynecol Obstet* 2018; **297**:257–267.

Wallace WH, Anderson RA, Irvine DS. Fertility preservation for young patients with cancer: who is at risk and what can be offered? *Lancet Oncol* 2005; **6**:209–218.

Wang Y, Yu A, Yu FX. The Hippo pathway in tissue homeostasis and regeneration. *Protein Cell* 2017; **8**:349–359.

Wang C, Zhu X, Feng W, Yu Y, Jeong K, Guo W, Lu Y, Mills GB. Verteporfin inhibits YAP function through up-regulating 14-3-3 σ sequestering YAP in the cytoplasm. *Am J Cancer Res* 2016; **15**:27–37.

Wei H, Wang F, Wang Y, Li T, Xiu P, Zhong J, Sun X, Li J. Verteporfin suppresses cell survival, angiogenesis and vasculogenic mimicry of pancreatic ductal adenocarcinoma via disrupting the YAP-TEAD complex. *Cancer Sci* 2017; **108**:478–487.

Westphal JR, Gerritse R, Braat DDM, Beerendonk CCM, Peek R. Complete protection against cryodamage of cryopreserved whole bovine and human ovaries using DMSO as a cryoprotectant. *J Assist Reprod Genet* 2017; **34**:1217–1229.

Yahng SA, Yoon JH, Shin SH, Lee SE, Cho BS, Eom KS, Kim YJ, Lee S, Kim HJ, Min CK et al. Influence of ex vivo purging with CliniMACS CD34(+) selection on outcome after autologous stem cell transplantation in non-Hodgkin lymphoma. *Br J Haematol* 2014; **164**:555–564.

Zhou L, You JH, Wu W, Li JM, Shen ZX, Wang AH. Pregnancies in patients with chronic myeloid leukemia treated with tyrosine kinase inhibitor. *Leuk Res* 2013; **37**:1216–1221.